An Active Artificial Iris Controlled by a 25-µW Flexible Thin-Film Driver

Florian De Roose[12], Soeren Steudel[2], Kris Myny[2], Myriam Willegems[2], Steve Smout[2], Marc Ameys[2], Pawel E. Malinowski[2], Robert Gehlhaar[2], Radhika Poduval[23], Xinyu Chen[32], Jelle De Smet[32], Andrés Vásquez Quintero[23], Herbert De Smet[23], W. Dehaene[12], and Jan Genoe[21]
[1]KULeuven, Leuven, Belgium, email: florian.deroose@imec.be
[2]imec, Leuven, Belgium, [3]UGent, Gent, Belgium

***Abstract*—**We show an active artificial iris based on solely thin-film components, wherein several LCD elements are controlled a metal-oxide TFT and by powered by thin-film photovoltaics (TFPV). Key aspects for the driver are size and low power consumption. We demonstrate power consumption down to 25µW for the full iris.

I. Introduction

The iris is a vital part of the eye, modulating the amount of light reaching the retina. An estimated 200,000 individuals worldwide suffer from some form of iris deficiency, with great discomfort and extreme photosensitivity [1]. Examples are aniridia and leiomyoma (Fig. 1).

To address this issue, active modulation of pupil diameter is required with minimized invasiveness. For this, a smart contact lens seems as an ideal solution. Smart lenses are shown with limited functionality, even in research. Global research aims to integrate active electrical and optical components in one platform, with possible components illustrated in Fig. 2 [2]. Here we focus on the active artificial iris (AAI).

The prospect of using liquid crystal display (LCD) capable of electro-optic actuation as a surrogate iris was explored by H. De Smet et al [3,4]. A prototype of this LCD setup was recently implemented on a spherically-conformal polymer surface, in the form of distinct rings with electo-optically actuatable opacity as shown in Fig. 3 [3]. In order to transform this device into a commercial application, several challenges need to be addressed, ranging from integrating a driver, to process technology, to all kinds of biocompatibility issues. This paper discusses the integration of a flexible driver on the lens with LCD.

II. Powering Scheme

There are several options to power a smart contact lens, as can be seen in Fig. 4. Options range from RF wireless power transfer [5], batteries, biofuel cells [6] through thin-film photovoltaic (TFPV) cells [7] in a miniaturized module. For the purpose of the active artificial iris, the use of an organic thin-film photovoltaic is preferred. It provides convenient integration in a flexible platform and simultaneously operates as an integrated illumination sensor.
Fig. 5 shows the full integration layout of the AAI concept. The inner three rings are used as separate LCD sections that are turned on sequentially by the TFT drive, when more light is available. The area exterior to the largest ring can be used for placing the driver electronics, which should be as small as possible. The rest of the area can be filled with TFPV. Our first steps in this regard can be seen in Fig. 6, showing the JV curves for a 10 subcell minimodule, with efficiencies above 3%. The device used is an organic thin-film photovoltaic structure using pDPP5T-2. The module is designed to generate an open circuit voltage of around 5V.
Fig. 7 shows the ideal iris performance based on measurements on humans [8], as well as the best possible approximation given the three LCD sections of Fig. 5. It also indicates the amount of power available. Notice that due to the logarithmic scale of the light intensity, only power in the nanowatt range is available at the first switching point. Due to the switching requirements of the LCDs, it is not possible to switch on the outer circle, which will mean poorer vision in dark environments. Furthermore, Fig. 7 illustrates that the driving electronics needs to be extremely power efficient.

III. Circuit Technology and Driver Requirements

As shown in Fig. 8, the LCD has a few requirements which have to be addressed by the driver chip. In order to operate properly, the LCDs need an alternating voltage with zero bias and a swing of at least 3V RMS in order to turn fully opaque. The alternation frequency has to be higher than 100Hz to avoid visible flickering. The estimated capacitance of all rings together is around 180pF. Finally, the driver substrate needs to be flexible, and the size as small as possible and banana shaped to fit the electronics on the lens, as shown in Fig. 5.

For the driver technology, we selected the amorphous indium gallium zinc oxide (a-IGZO) self-aligned thin-film transistor (TFT) on polyimide technology of imec [9,11], because of its high performance and reproducibility. The circuits are n-type only, with the basic transistor building block explained in Fig. 9. This variation is a circuit stack, which is characterised by thin gate dielectric for best channel control and a thick intermetal dielectric for small overlap capacitances. Fig. 10 shows the transfer characteristics of the TFTs for several channel widths. Notice that the V_T of the technology is slightly negative, resulting in a leakage current, even when V_{GS}=0V. Going to small widths is essential for low power design, since the power consumption scales linearly with the minimal width (5µm used in this design). In Fig. 11, a significant variability of the technology is illustrated. All designs in this technology have to be resilient to up to 0.5V for ΔV_T. Finally, Fig. 12 shows that the transparency of the complete circuit on foil is above 50%, giving a possibility of adding circuitry in the entire perimeter of the contact lens without significant loss of vision.

IV. Driver design

This section describes the design of a driver for the LCD using as little power as possible, and turning on at the appropriate moment, which is determined by the available incident illumination. The general overview of the driver is shown in Fig. 13. It consists of an oscillator to generate the alternating signal, and an H-bridge driven by this signal to charge and discharge the plates of the LCD capacitor.

Fig. 14 shows the detailed implementation of the oscillator. We used a ring oscillator because of its simplicity and limited number of components, which will result in small power consumption.

Pseudo CMOS is used as the logic configuration [10], since it is a robust style which can handle both positive and negative values of V_T. As disadvantages, it has high power consumption due to the first stage which draws static power (worse for lower V_T) and has a large footprint due to four transistor per inverter. A more appropriate style for this application with lower power is dual V_T diode load inverter, but this requires a technology which can provide two types of TFTs, one with positive and one with negative V_T.

The number of stages in the ring oscillator is an optimization between the power consumption of the ring oscillator and the H-bridge with load capacitor. Having more stages will lead to more power consumption in the ring oscillator, since it is dominated by the leakage path in every stage, but it will also decrease the oscillation frequency. This in turn will reduce the power used by the H-bridge with load capacitor, since it is dominated by charge and discharge losses in the capacitor, which is linearly frequency dependent. For our application with a load between 30pF and 180pF, an 11-stage design was optimal.

Fig. 15 shows the H-bridge and load capacitor with the different sizes tested. Increasing the size of pull up (PU) and pull down (PD) transistor will decrease the rise and fall time at the capacitor, yielding larger RMS values, but also consumes more power due to the larger leakage current in the output stage, even without load.

V. Measurements

We have fabricated the devices described above and measured the output waveforms and power consumption for four variations. Fig. 16 shows the chip photograph (V1), the core area is only 0.75mm². The measured frequencies were very close to one another for all variations, independent of the output stage or its loading, and were between 300Hz and 600Hz. For power consumption and RMS value, both measurements without load and with 180pF load have been performed. Power consumption without load is a factor 4 lower than with the load, indicating that the capacitor consumes 75% of the energy. Furthermore, the power is lower with smaller output stages, as shown in Fig. 16. However, also the output RMS values are lower, requiring a higher supply to activate the LCDs. V1, with largest PU and PD TFTs, has with 25µW the lowest power consumption for 3V RMS swing under load, V4 has the largest with 30µW. With 25µW and the TFPV properties given in Fig. 5 and 6, this means the LCD will trigger at approximately 1/20 of 1 sun.

Finally we have connected the chip and the LCD together, as is shown in Fig. 17. For this experiment we used a man-shaped LCD rather than the concentric circles for demonstration purposes. Measurements show that the LCDs operate until the supply drops below 5V, at which point the oscillator also stops functioning.

VI. Conclusion

We have shown an active artificial iris concept using a thin-film photovoltaic minimodule as a power supply, a flexible thin-film circuit in a-IGZO technology as a driver chip and a liquid crystal display to act as the iris. We show very low power consumption down to 25µW for the driver chips. We finally show that the driver chip and the LC display can work together, and produce very promising results.

Acknowledgment

F. De Roose thanks the Agency for Innovation by Science and Technology in Flanders (IWT-Vlaanderen) for financial support. Furthermore, A. V. Quintero thanks the Swiss National Science Foundation (SNSF) for the Early PostDoc fellowship under the grant No. P2ELP1_158871.

References

[1] J. S. Glaser, "Neuro-ophthalmology", Harper and Row, 1977

[2] J. De Smet, "The Smart Contact Lens: from an Artificial Iris to a Contact Lens Display", *PhD Thesis*, UGent, 2014

[3] H. De Smet, *et al.*, "Curved Guest-Host LCD used as a dynamic artificial iris", in *SID-ME Chapter Spring Meeting 2014*, pp. 22, 2014

[4] J. de Smet *et al.*, "Design and Wrinkling behavior of a contact lens with an integrated liquid crystal light modulator ", Jnl Display Tech, vol, 8, 5, pp. 299-305, 2012

[5] G. Wang *et al.*, "A dual band wireless power and data telemetry for retinal prosthesis.", in *Conference Proceedings of IEEE Eng Med Soc 2006,* pp. 4392-4395, 2006

[6] M. Falk *et al.*, "Biofuel cell as a power source for electronic contact lenses", in *Biosensor and Bioelectronics*, vol. 31, pp 38-45, Sept 2012

[7] J. Tait *et al.*, "Determination of Solvent Systems for Blade Coating Thin Film Photovoltaics" in *Advanced Functional Materials*, vol. 25, pp 3393-3398, Jun 2015

[8] C.A. Blackie, H.C. Howland, "An extension of an accommodation and convergence model of emmetropization to include the effects of illumination intensity", in *Ophthalmic Physiological Optics*, vol. 19, pp. 112-125, Mar 1999

[9] M. Nag *et al.*, "Flexible AMOLED Display and Gate-driver with Self-aligned IGZO TFT on Plastic Foil" in *SID international symposium 2014: digest of technical papers*, pp. 248-251, Jun 2014

[10] T.-C. Huang *et al.*, "Pseudo-CMOS: A Design Style for Low-Cost and Robust Flexible Electronics" in *IEEE Transactions on Electron Devices*, vol. 58, pp 141-150, Nov 2010

[11] F. De Roose *et al.*, "A flexible Thin-Film Pixel Array with a Charge-to-Current Gain of 59µA/pC and 0.33% Nonlinearity and a Cost Effective Readout Circuit for Large-Area X-ray Imaging", in *Proceedings of ISSCC 2016*, pp.296-297, Feb 2016

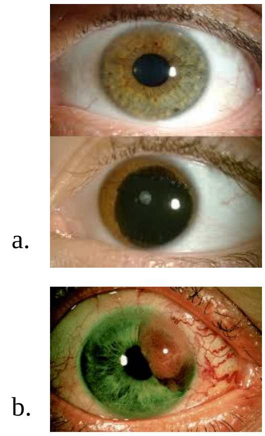

Fig. 1: Aniridia (a) and iris leiomyoma (b) are pathologies that can be helped by an artificial iris.

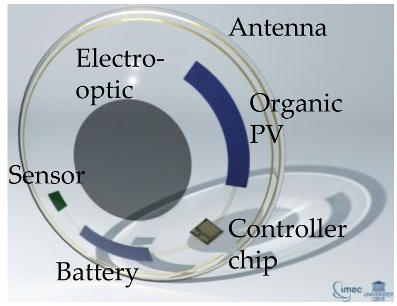

Fig. 2: An ideal smart contact lens with integrated display, energy harvesting, communication antenna sensors and more.

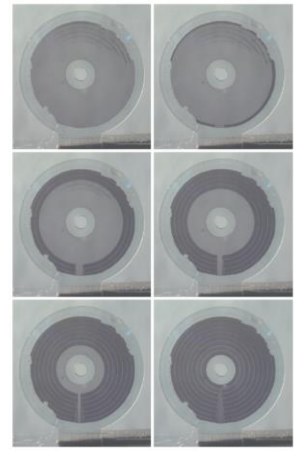

Fig. 3: Technology for making the individual liquid crystal (LC) rings used as an iris. More detail in [2].

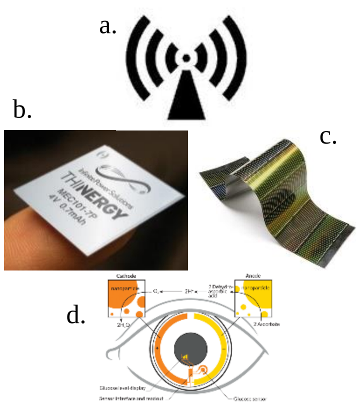

Fig. 4: Options for powering a smart contact lens: a. wireless (eg. NFC), b. thin battery, c. thin-film photovoltaics, d. biofuel cells [6].

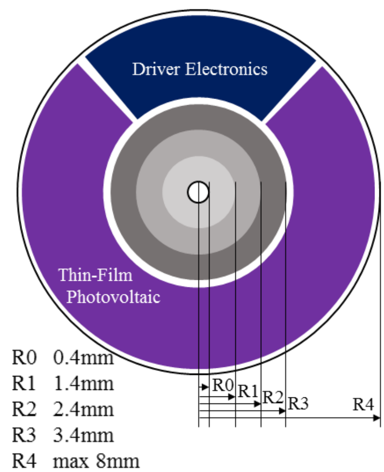

Fig. 5: Overview of the components of the AAI. The middle rings are LCD elements, the other area is for driver electronics and energy harvesting.

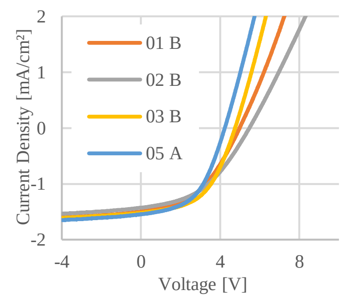

Sample	J_{SC} (mA/cm²)	V_{OC} (V)	FF (%)	η (%)
01 B	1.50	4.99	44.4	3.4
02 B	1.43	5.48	43.6	3.5
03 B	1.52	4.76	50.9	3.7
05 A	1.54	4.24	50.4	3.3

Fig. 6: JV curve of the thin film photovoltaic module for the fully integrated project. Around 15 cells in series are required for 5V output at MPP.

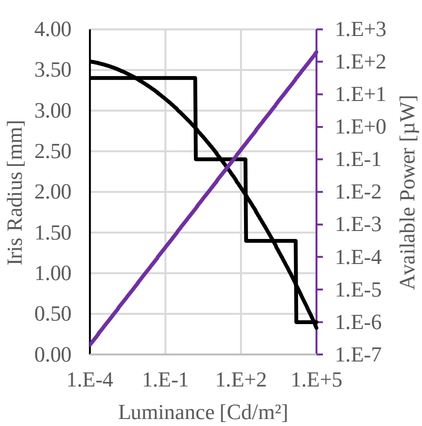

Fig. 7: Ideal human iris radius according to [8] and approximated radius by the artificial iris, and the power generated by the thin-film photovoltaics.

LCD thickness	9µm
Capacity R2-3	90pF
Capacity R0-1	27.8pF
Voltage swing	min +5V ... -5V, zero reference to avoid LC degradation
Frequency	100Hz ... 1000Hz
Substrate	Flexible, ideally bendable
Size	As small as possible Banana shaped

Fig. 8: List of requirements for the driver chip, imposed by the LC rings.

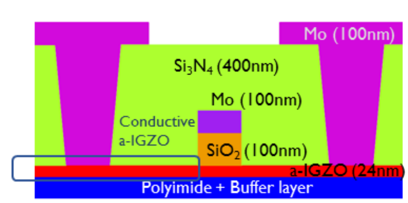

Fig. 9: Cross section of the a-IGZO technology used for the driver chip [11].

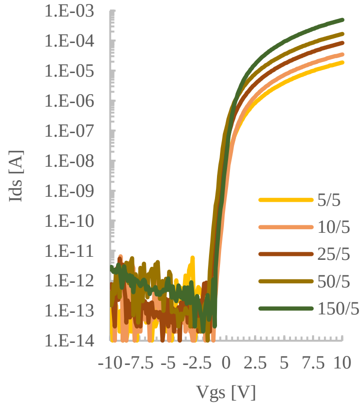

Fig. 10: Transfer characteristics of the TFTs, showing the scaling of W. Small W is essential for low power operation.

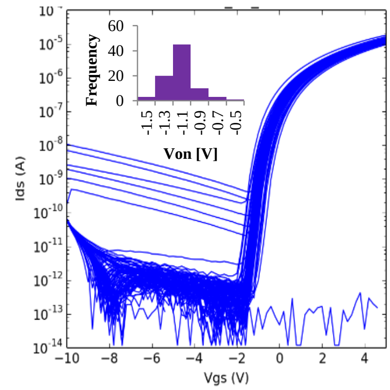

Fig. 11: Variability for the self-aligned technology for a 15µm/5µm TFT. Any design needs to be very resilient to parameter variations.

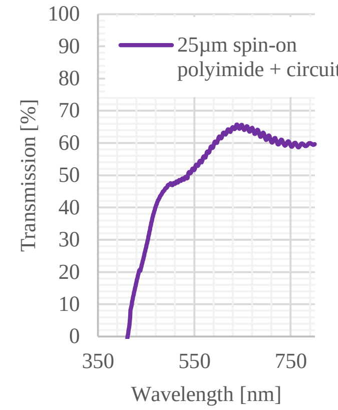

Fig. 12: Transparency of the circuit technology without the carrier glass wafer. A significant portion of light is still transmitted through it.

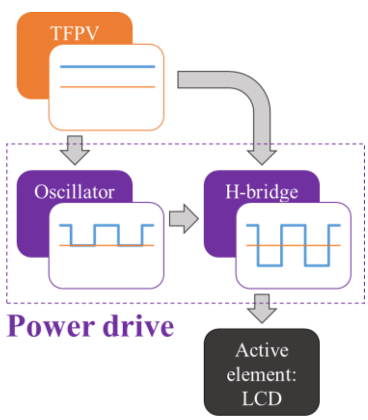

Fig. 13: Overview schematics of the artificial iris driver. For delivering the high power to the LCD, an H-bridge is used.

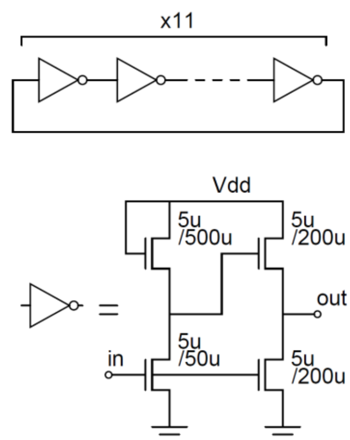

Fig. 14: Detailed schematic of the ring oscillator, using pseudo CMOS inverters used on one supply rail.

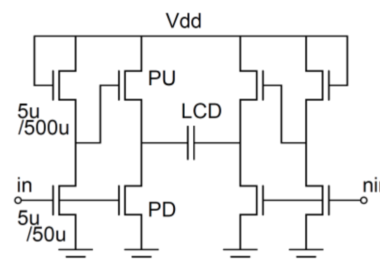

	PD	PU
V1	40µm	160µm
V2	40µm	80µm
V3	20µm	80µm
V4	20µm	40µm

Fig. 15: Detailed schematic of the H-bridge, with different variations of the push-pull stage.

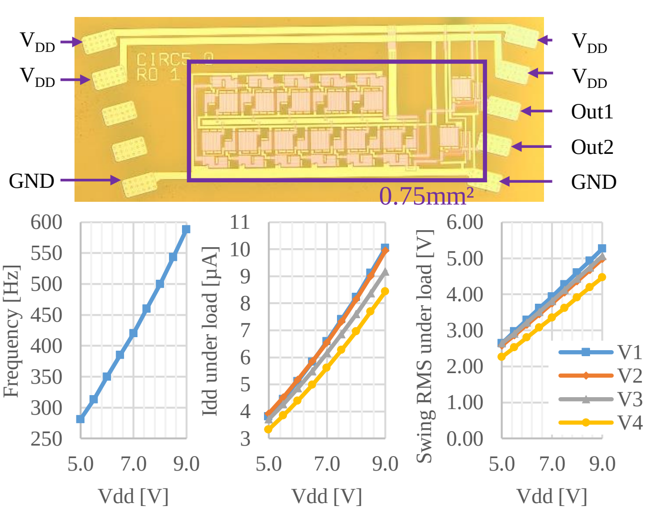

Fig. 16: Chip layout and performance characteristics, showing oscillation speed and power consumption and RMS swing under 180pF.

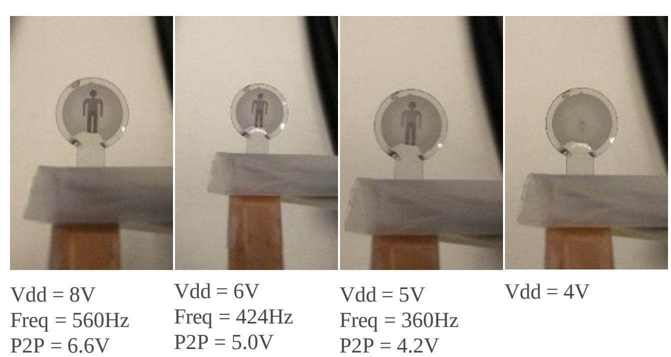

Fig. 17: Measurement of the integrated system of driver chip and LCD. The LCD becomes transparent if the supply drops below 5V. For demonstration purposes the electrodes are man-shaped.